


RESEARCH

Open Access



# Double-edged sword of biofouling potentials associated with haemocompatibility behaviour: titania nanotube arrays for medical implant surface technology

Keethanjali Palaniyappan<sup>1</sup>, Rabiatul Basria S. M. N. Mydin<sup>1\*</sup> , Darius Widera<sup>2</sup>, Siti Salmah Noordin<sup>3</sup>, Nor Hazliana Harun<sup>1,4</sup>, Wan Nuramiera Wan Eddis Effendy<sup>1</sup>, Roshasnorlyza Hazan<sup>5</sup> and Srimala Sreekantan<sup>6</sup>

## Abstract

**Background** Medical implant failures are frequently associated with limitations of the surface technology that lead to biofouling and haemocompatibility issues. Titania nanotube array technology could provide a solution for this existing limitation. The present study describes the biofouling potential using the simulated body fluid model according to ISO 23317-2007 and haemocompatibility profiles according to ISO 10993-4 guidelines. Further haemocompatibility profiles were also assessed by evaluating full blood count, coagulation assays, haemolytic rate, whole blood clotting factor, platelet profiles, and FESEM characterization.

**Result** Titania nanotube array nanosurface was found to present with better apatite biofouling and hydrophilic potential compared to bare titanium foil. Furthermore, good compatibility behaviour was observed based on the haemocompatibility profiles where no signs of thrombogenesis and haemolysis risks were observed. Titania nanotube array reduced fibrinogen adsorption, red blood cell and platelet adhesion and activation, which could be associated with detrimental biofouling properties.

**Conclusion** Titania nanotube array could possess a double-edged sword of biofouling potentials that resist detrimental biofouling properties associated with thrombogenesis and haemolysis risk. It also provides better apatite biofouling potential for improved tissue and osseointegration activities. Knowledge from this study provides a better understanding of medical implant surface technology.

**Keywords** Titanium dioxide nanotube arrays, TiO<sub>2</sub> nanotube arrays, Surface technology, Medical device, Biofouling, Medical implant

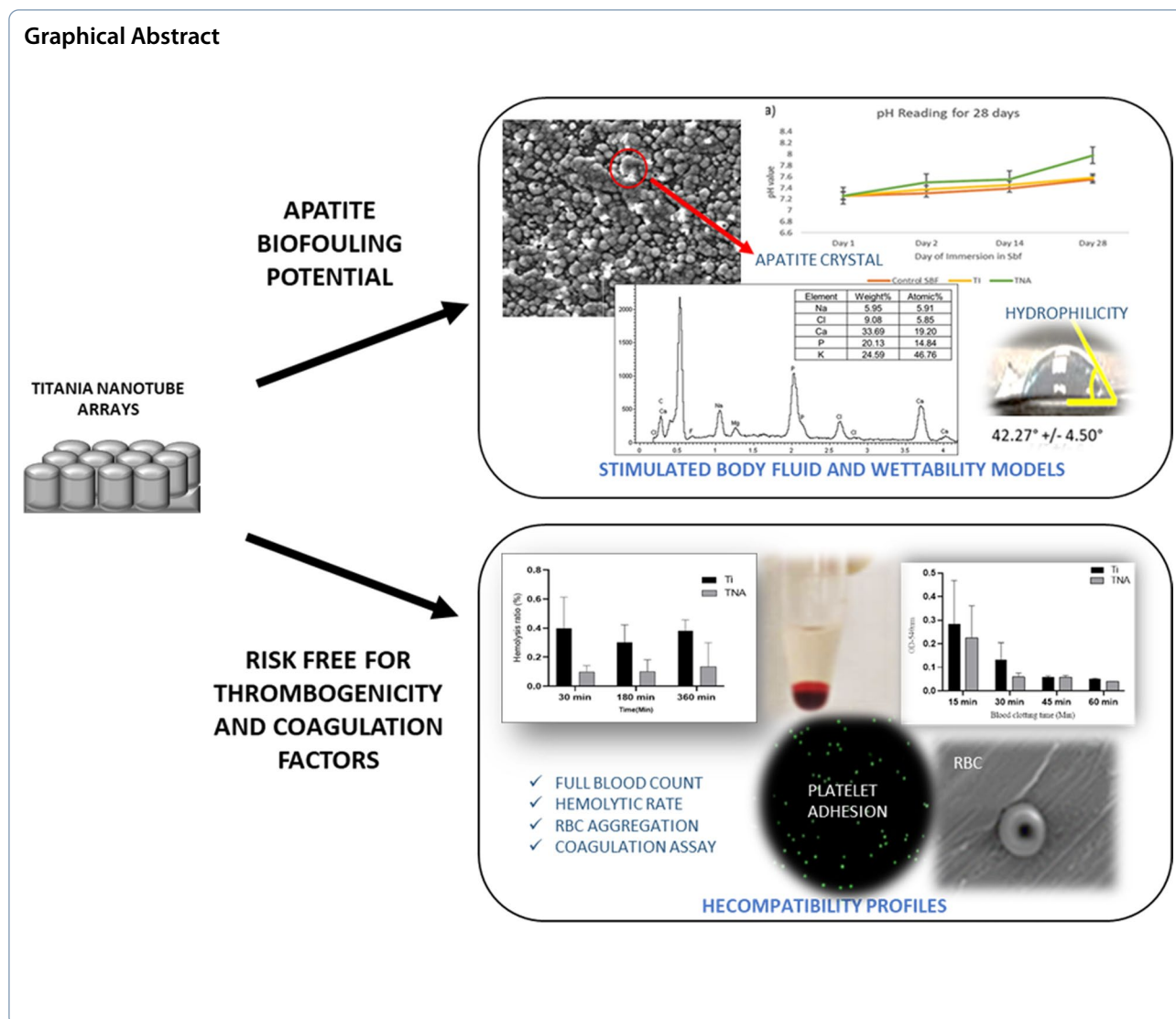
\*Correspondence:

Rabiatul Basria S. M. N. Mydin  
rabiatulbasria@usm.my

Full list of author information is available at the end of the article



© The Author(s) 2023. **Open Access** This article is licensed under a Creative Commons Attribution 4.0 International License, which permits use, sharing, adaptation, distribution and reproduction in any medium or format, as long as you give appropriate credit to the original author(s) and the source, provide a link to the Creative Commons licence, and indicate if changes were made. The images or other third party material in this article are included in the article's Creative Commons licence, unless indicated otherwise in a credit line to the material. If material is not included in the article's Creative Commons licence and your intended use is not permitted by statutory regulation or exceeds the permitted use, you will need to obtain permission directly from the copyright holder. To view a copy of this licence, visit <http://creativecommons.org/licenses/by/4.0/>.



### 1 Background

Biofouling and haemocompatibility properties of the implantable surface are still major challenges in medical implant technology. Biofouling is the term to describe the deposition of any biological material on a surface. The biofouling potential of blood-contacting medical devices commonly involves proteins, and some other body fluid inside the body, besides human tissues or bone cells [10]. Thrombogenesis and haemolysis are common issues related to medical implantation failures. The interfacial of implantable medical surfaces is associated with highlights and challenges for biofouling, especially in terms of material efficacy [20]. Implant failure often associated with platelet biofouling could negatively trigger coagulation and

thrombogenesis activities [24]. On the other hand, a good blood-contact medical implant should not have any unfavourable interactions with blood components. Therefore, the present work provides further understanding of nanosurface technology with biofouling potential using simulated body fluid (SBF) model and human blood for haemocompatibility profiles according to ISO10993-4 guidelines. Knowledge from this work could contribute significantly to medical implant surface technology, especially regarding titania nanotube arrays (TNAs). TNA has become widely been studies for medical implants technology, especially for orthopaedics and dental applications [16, 27]. Present study provides an overview of the double-edged sword of biofouling potential TNA that associated with haemocompatibility behaviour.

## 2 Methodology

### 2.1 Sample preparation

The titanium foil (Ti) was purchased from Strem Chemical Inc, the USA, with 0.13 mm thickness and 99.7% purity, while the glass slide, which served as control, was obtained from Sigma-Aldrich, USA. The TNA nanosurface was produced according to our previous work (Effendy [11]; Mydin [27]). In brief, the Ti was anodized in fluoride salts and organic electrolyte solution and subjected for annealing with argon gas to generate anatase crystal structure.

### 2.2 Simulating body fluid model

Simulating body fluid (SBF) solution mimics human blood plasma medium, which contains ions concentration, especially on the apatite nucleation model. In this study, the SBF solution was prepared according to the standard procedure as stated in the paper of Oyane et al. [28]. The sample with the size of  $1 \times 1$  cm was immersed into the solution for the selected period. Data were recorded for day 1, day 2, day 14, and day 28 for weight changes and pH changes. Apatite formation observation was examined through field emission scanning electron microscope (FESEM) for 28-day incubation period. Samples were coated with platinum and observed under an accelerating voltage of 5 kV (FESEM, LEO GEMINI, Carl Zeiss, Oberkochen, Germany). For Inductively coupled plasma-optical emission spectrometry (ICP-OES) done according to ISO 23317-2007 guidelines, data were collected on day 28 exposure and normalized with blank of the same studied period. Sodium (Na), potassium (K), phosphorus (P), and calcium (Ca) were ions selected for the study due to their importance in apatite formation [2].

### 2.3 Wettability

The sessile drop method was used to measure the contact angle ( $T$ ) with a goniometer as described by Schuster et al. [31]. A total of 20  $\mu$ L of sterile deionized water was dropped on top of the sample surface, and five angles of wettability were captured and measured. The photograph was then processed using Image J software and was statistically analysed by paired  $t$ -test and presented as mean  $\pm$  SD for each sample.

### 2.4 Haemocompatibility profiles

The approach described in the International Standard Organization (ISO 10993-4) was used to assess the haemocompatibility profile including the thrombogenicity and haemolytic potential. All studies were carried out in triplicate systems. Blood samples were collected in anticoagulant tubes containing ethylene diamine

tetra-acetic acid (EDTA) for full blood count and haemolytic testing, while a 3.2% buffered sodium citrate anticoagulant tube was used for thrombogenic assays.

### 2.5 Full blood count

The full blood count (FBC) on 3 mL of a blood sample using haematology analyser (CELL-DYN Ruby Haematology Analyzer, Abbott, Myanmar) from each volunteer ( $n=3$ ) was done after exposure with Ti alloy and TNA nanosurface samples in the size of  $3 \times 2$  cm. The parameters observed were the total red blood cell, haemoglobin (Hb), haematocrit (PCV), mean cell volume (MCV), mean corpuscular haemoglobin (MCH), mean corpuscular haemoglobin concentration (MCHC), total white blood cell, and platelet count. Blood without exposure to any samples represents a control for FBC parameters [3].

### 2.6 Coagulation assays (activated partial thromboplastin clotting time and prothrombin time)

Blood sample was obtained from each volunteer ( $n=3$ ) in an anticoagulant tube containing 3.2% sodium citrate. Then, the materials in the size of  $3 \times 2$  cm were taken out of the phosphate-buffered saline (PBS) and immersed straight into the blood tube. The tube was gently tilted to allow the surface of the substance to come into touch with the blood. The tube was subsequently packaged and delivered to the BP Penang laboratory for an automatic clotting tester (Automated Coagulation Analyzer—Dt 100, T-Coag, Ireland). The duration of blood clotting time was performed on blood that had been exposed to the material and blood that had not been exposed to the substance as a control.

### 2.7 Haemolysis rate

The testing film ( $0.5 \text{ cm} \times 0.5 \text{ cm}$ ) was incubated with PBS in a centrifuge tube. Then, whole blood from the EDTA tube was added and incubated at  $37^\circ\text{C}$  for 30 min, 3 h, and 6 h. Triton X-100 (1%) and saline were employed as positive and negative control. After the indicated incubation period, the tube was centrifuged for 5 min at 2500 rpm. The supernatant was measured by the optical densities (OD) at the wavelength of 540 nm using a UV spectrophotometer. The percentage of haemolysis was calculated as the formula:  $\text{HR} (\%) = (D_t - D_{nc}) / (D_{pc} - D_{nc}) \times 100\%$ , where HR is the haemolysis ratio and  $D_t$ ,  $D_{nc}$ , and  $D_{pc}$  are the absorbance of test samples, negative controls, and positive controls, respectively [25, 32].

### 2.8 Whole blood kinetic clotting time measurement

Blood without anticoagulant was pipetted on the materials' surface ( $1 \times 1 \text{ cm}$ ) and was allowed to coagulate for

15, 30, 45, and 60 min. Following the interval, 500  $\mu$ l of distilled water was poured into the well's surroundings being immersed in distilled water for 5 min to lyse. The amount of free haemoglobin released was determined using a plate reader with a wavelength of 540 nm [30]. The free haemoglobin concentration provides a correlation to the extent of blood clotting, with larger amounts of free haemoglobin indicating less clot formation on the substrates.

### 2.9 Platelet adhesion

To extract platelet-rich plasma (PRP), whole blood was collected in 3.2% buffered sodium citrate and centrifuged at 3000 rpm for 15 min. Following centrifugation, 0.1 ml of PRP was applied to the study surface (Ti alloy and TNA nanosurface) in 96-well plates and incubated at 37 °C for 1 h in a static environment. The sample was washed with PBS after the incubation time and was then stained with Calcein AM and examined under a fluorescence microscope [14]. Three images were collected for each surface with a 10 $\times$  objective lens, and those images were quantitated using Image J imaging software.

### 2.10 FESEM for whole blood and platelet activation

The materials were incubated for 1 h at 37 °C with 100  $\mu$ l of PRP for platelet activation analysis and 100  $\mu$ l of RBC for RBC aggregation test. The sample was then gently rinsed twice with PBS before being fixated for 2 h at room temperature with a 2.5% glutaraldehyde solution. Fixed samples were dehydrated using a series of ethanol soaks of 50%, 70%, 80%, 95% ethanol, and 100% ethanol. Following materials will be dried for 15 min and kept frozen at -20 °C until FESEM screening sputtered with platinum and captured with a 5-kV accelerating voltage.

### 2.11 Statistical analysis

The experiments were carried out in triplicate, and the statistics were analysed using two-way ANOVA in the SPSS software for Windows (version 27.0, IBM Corporation, USA). All the data were presented as mean  $\pm$  standard deviation. The results were considered significant when the *p*-value is < 0.05.

## 3 Results

### 3.1 Apatite biofouling potential

In this study, the apatite formation capability can initially be observed by SBF pH changes. The pH of both Ti and TNA were increased consistently from day 1 to day 28 (Fig. 1). However, there are no significant changes observed on weight different the pre- and post-immersion of the samples at milligram (mg) level.

Further observation on TNA nanosurface using FESEM showed better biofouling capability of apatite

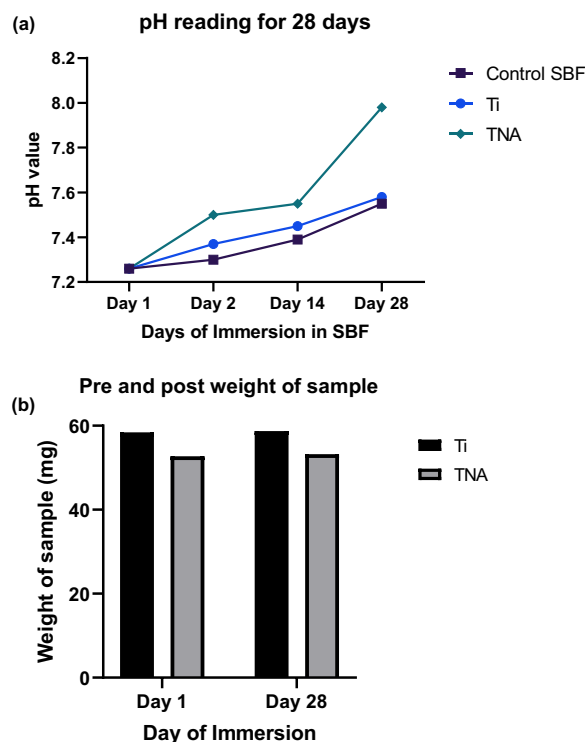


**Fig. 1** Apatite formation ability for 28 days profiles on Ti and TNA using SBF model. **a** pH reading from day 1 to day 28 profile. **b** Pre & post-weight changes on day 1 and day 28 profile

crystal layer-clustered ball-like particles with a mean size of about 1.5  $\mu$ m (red circle indicator in Fig. 2) compared with Ti alloy (without nanosurface) after 28 days of immersion period in SBF. The EDX element analysis indicates the presence of elements such as Na, Cl, and C for Ti alloy, while Na, Ca, P, K, and Cl on the TNA nanosurface. TNA nanosurface showed the presence of higher elements on its surface in comparison with Ti alloy. Furthermore, TNA present with better surface roughness that could enhance apatite biofouling activity on its nanosurface is observed in Fig. 2B.

The apatite biofouling potential on TNA nanosurface was further studied by ICP-OES as tabulated in Table 1. As presented in Table 1, Na levels were found to be significantly higher in buffers containing TNA ( $p = < 0.0001$ ) on d-28. However, for P an Ca ion is undetectable possibly due to limitation in study sample volume. There are about fourfold increments  $120.50 \pm 1.52$  mg/mL on day 28 which Na content may benefit the TNA nanosurface in haemocompatibility functionality compared to Ti alloy and it is significant where the *p*-value is 0.0375.

Another key element for biofouling ability on any implantable surface can be described by the wettability (WCA) properties. Figure 3 shows that the wettability



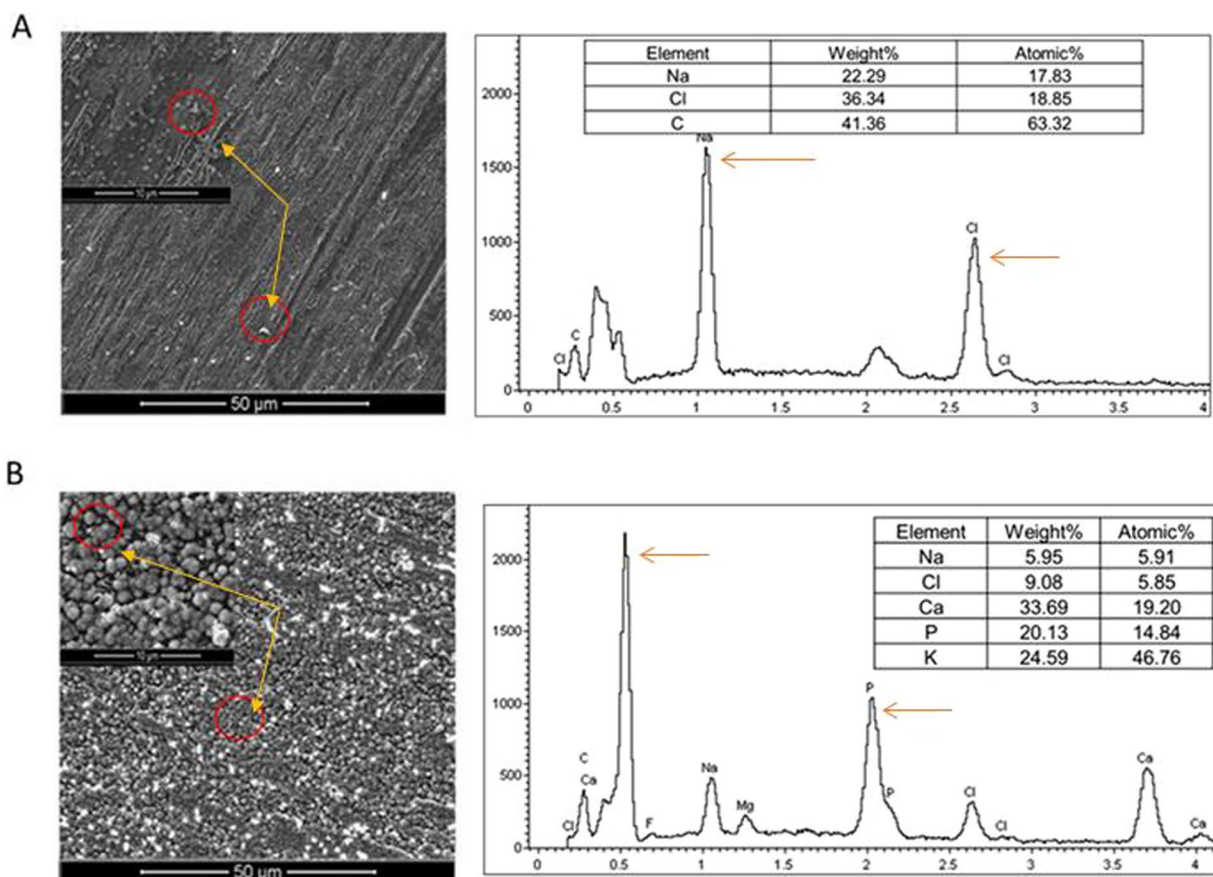


**Fig. 2** FESEM and EDX profiles of apatite crystal formation on Ti alloy and TNA surface at 28-day immersion period in SBF. **A** apatite formation on TNA nanosurface with EDX profiles **B** apatite formation on Ti alloy without nanosurface with EDX profiles. The image was captured under magnification of 2000× (50 μm) and 10,000× (10 μm)

**Table 1** Total ion contents using ICP-OES

Sample	Day	Total ion content (s) (mg/mL)	
		Na	K
Ti	28	36.00 ± 0.76	0.00 ± 0.48
TNA	28	120.50 ± 1.52	2.69 ± 1.52

Release of Na and K was measured for the Ti alloy and also TNA nanosurface in SBF after 28 days of immersion

properties of Ti and TNA were significantly ( $p = 0.017$ ) less than 90° and within hydrophilic range value. However, TNA is present with less WCA angle that suggests better hydrophilic behaviour compared to Ti. According to the research done by Chou [10] stated that an implant material should not be hydrophobic so it can be resistant to interaction with the surrounding environment, enhance hydrogen bonding and be anti-fouling. In this study, TNA nanosurface showed hydrophilic

properties which could allow finer hydrogen bonding and appetite formation abilities.

### 3.2 Haemocompatibility potential

The preliminary observation on the ex vivo full blood count profile is shown in Table 2. There are not many noticeable changes in the value of the parameters before and after the immersion of study samples, especially TNA nanosurface. In this study, RBC values were constant upon interaction with Ti and TNA for all three patients possibly with no sign of haemolysis activity (Fig. 4). The platelet count was constant for both samples in our investigation. Thus, finding from this study suggests that there is no indication of haemolysis or changes in platelet count indicating the haemocompatibility potential.

TNA nanosurface was further tested for anti-coagulant properties as shown in Table 3. The results of the PT and APTT tests were compared with those of the untreated sample, which consist of blood without incubated

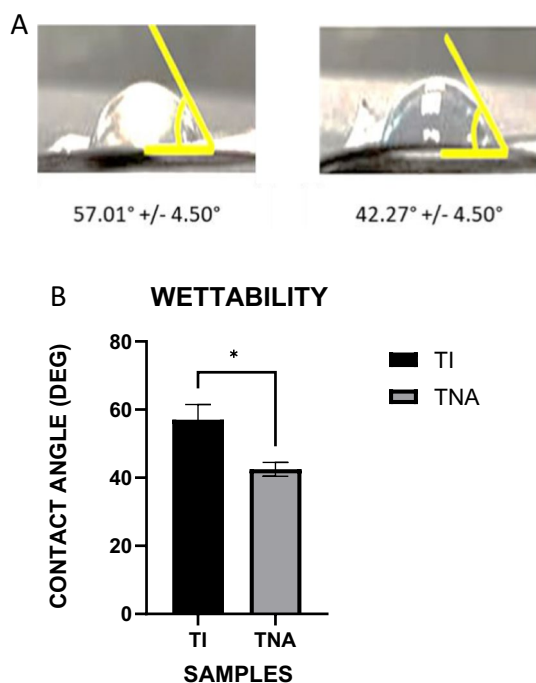


**Fig. 3** Wettability analysis by ImageJ software on the droplet of water on each tested sample. **A** Image of a droplet of water on the sample Ti and TNA. **B** histogram of the contact angle values of the wettability profile on surface of Ti and TNA on foil substrate suggests the surfaces presented with hydrophilic properties, WCA < 90°, n = 3. Data were expressed as mean ± standard deviation as error bar

samples. The result shows the surface TNA shows reduction in the time of clotting for both PT and APTT. Ti, on the other hand, presents with prolonged time for PT and APTT. These findings suggest that the tendency for activating blood coagulation factors is lower on TNA compared to Ti surface.

Further observation on the haemolytic rates described that both the samples for all three periods were between 0 and 0.4% (Fig 4). According to the ASTM F756-08 [1] standard, the materials with a haemolysis rate lower than 2% are classified as haemocompatible, which does not involve haemolytic activity and damage the blood red cells. TNA nanosurface excelled Ti alloy in terms of haemolytic rate, with a rate of less than 0.2% for all three time periods in this investigation.

The whole blood clot kinetic test is described in Fig. 5. The whole blood clotting kinetic is mainly used to assess the haemostatic performance of material when in contact with the blood surfaces. From the data obtained, there is a significant difference between the material’s surface of Ti alloy and TNA nanosurface for times 15, 30, 45, and 60 min. For Ti, when we compare the OD of 15 and 30 min, the significant whole blood kinetic was observed  $p=0.0014$ , while for TNA the value was  $p=0.0012$ .

In general, by comparing both materials, TNA shows a better result in releasing the low amount of free haemoglobin by expressing a low OD value after 30 min. In the graph shown, the release on the surface of TNA, the haemoglobin stopped at minute 30 and formed a whole blood clot while comparing to Ti where the release was continuing till minute 45. The results indicate that blood clotting was significantly delayed on the Ti alloy in comparison with the TNA nanosurface.

Platelet adhesion profile is described in Fig. 6. Platelet adhesion is the indication for the presence of thrombogenicity of the implantable surface used. In this study, the outcome of platelet adherence on the surface of the material examined after it was treated with calcein AM and screened using a fluorescence microscope. In this study, it is demonstrated that TNA nanosurface has lesser fibrinogen adsorption, as evidenced by the low presence of platelets on the material’s surface, as compared to Ti alloy without nanosurfaces and glass surfaces, which were utilized as controls.

For the red blood cell aggregation, TNA nanosurface showed a reduction compared to the surface of Ti alloy. From Fig. 7a, b, it can be seen that the shape of the cell is not destructed where it is presented in the biconcave disc. Both sides of the cell were curved perfectly without any evidence of rupture, which shows the surface does not cause any haemolysis to the red blood cell. There is also no sign of agglutination presence on both Ti and TNA surfaces; the cells were present in single-cell morphology where there is no harm can be seen. The FESEM picture of there is a presence of platelet on the TNA nanosurface; there is no trace of dendrites to leucocyte aggregations while Ti alloy reveals the existence of active platelets but no evidence of dendrites and shows there is no evidence of platelet activation on the surface of the materials. Hence, it is proven that the material shows no sign of thrombogenicity and can be classified as non-thrombogenic for both Ti and TNA surfaces.

#### 4 Discussion

Biofouling issues related to implantable medical devices are related to the interfaces between implant surfaces and host interaction, particularly in terms of efficacy and safety. Biofouling of biological molecules on an immobile surface will result in random, directed adhesion forces or lateral friction forces. The positive biofouling potential of implantable devices can be described by apatite formation ability. The degree of apatite biofouling on any implantable surface could contribute in better osseointegration activity in future as discussed by Khandan [18] and Oyane et al. [28]. The amount of apatite production on a surface is related to increased bioactivity and new

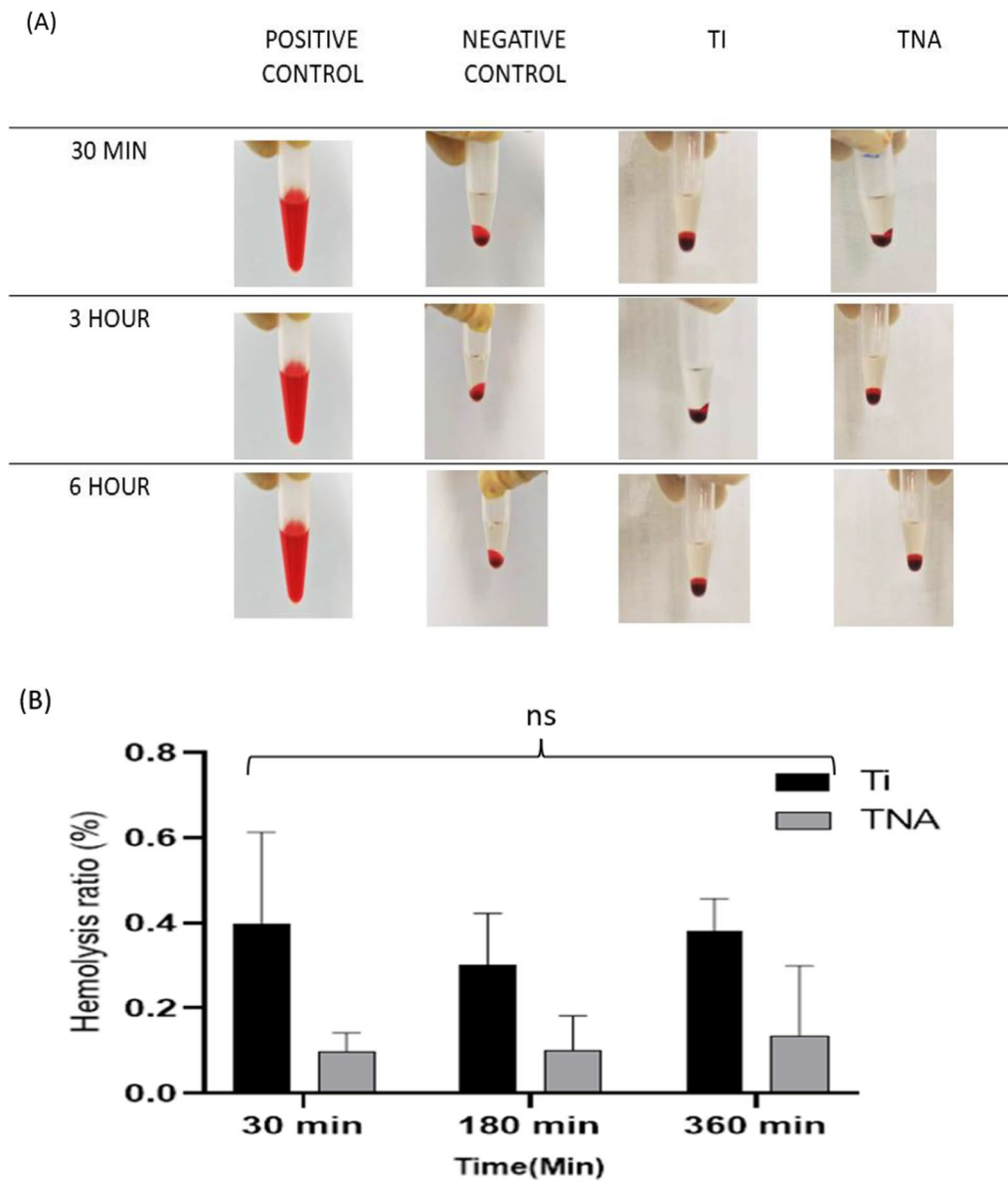


**Fig. 4** **A** Haemolytic assay of Ti and TNA surfaces. Image of samples after the centrifugation at 2500 rpm for 5 min. The presence of haemolysis in the supernatant is only observed in the positive control tube. **B** Haemolysis ratio profile of Ti and TNA surfaces. Results indicate there is no significant differences in all the period tested which is 30, 180 and 360 min which compared for both material surfaces (Ti and TNA) where the *p*-value is > 0.05. The error bar represents mean ± standard deviation in triplicate within three donors

bone formation ability. In this study, the roughness of the TNA surface improves the apatite biofouling properties and thus could be extremely advantageous for the production of osseous tissues [22]. According to the research done by Chou [10] stated that an implantable material surface should not be hydrophobic and resistant to surrounding environment interaction. In this study, TNA nanosurface showed hydrophilic properties

which could allow finer hydrogen bonding in apatite biofouling abilities .

As described by Kokubo [19], the release of cations observed in this study and the increase of pH in SBF solution could suggest the presence of an enhanced degree of apatite biofouling properties. The bone-binding elements usually take 28 days to form an appetite on the

**Table 2** Full blood count profile using ex vivo approaches

Full blood count	Average value (mg/dl)		
	Untreated	Ti	TNA
Total RBC	4.95 ± 0.78	4.95 ± 0.78	5.00 ± 0.71
Haemoglobin	142.00 ± 21.21	141.50 ± 21.92	142.00 ± 19.80
Haematocrit	0.44 ± 0.05	0.45 ± 0.07	0.46 ± 0.06
MCV	92.05 ± 1.61	90.91 ± 0.00	91.01 ± 0.14
MCH	28.71 ± 0.22	28.60 ± 0.06	28.40 ± 0.06
MCHC	311.90 ± 2.97	314.50 ± 0.71	312.10 ± 0.14
RDW	12.15 ± 0.49	12.15 ± 0.64	12.20 ± 0.57
Total WBC	5.73 ± 4.70	5.54 ± 4.52	5.94 ± 4.70

Results indicate mean values ± SD from 3 different donors for the parameters of full blood count

**Table 3** PT and APTT profiles

Coagulation assay	AVERAGE (time in seconds)		
	Untreated	Ti	TNA
PT	12.80 ± 0.45	13.57 ± 2.21	12.23 ± 0.67
APTT	35.77 ± 3.16	37.57 ± 4.97	36.40 ± 2.92

Results indicate mean values ± SD from 3 different donors for the coagulation assays

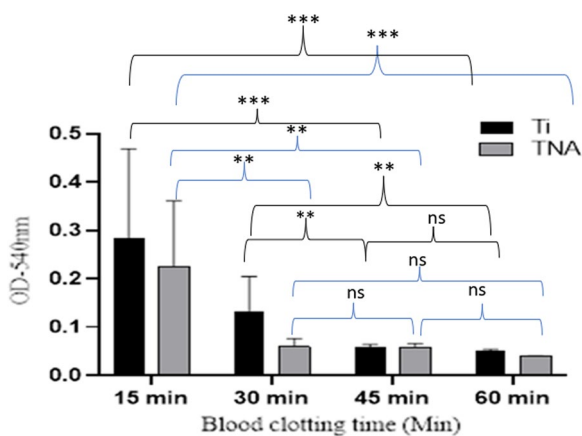


**Fig. 5** Whole blood kinetic profile for Ti and TNA surfaces. The findings demonstrate that there is a significant difference between the material’s surface of Ti alloy and TNA nanosurface for times 15, 30, 45, and 60 min where the *p*-value is less than 0.05 when compared with minute of 15 with 30, 30 with 45 min for both Ti and TNA. The error bar reflects the mean ± standard deviation for three donors’ triplicates

surface of a material. Furthermore, sodium ions (Na+) were released by exchange with H<sup>3</sup>O<sup>+</sup> ions, and this may cause the creation of a Ti–OH layer, which has a negative charge that will react electrostatically with the Ca<sup>+2</sup>

ions, which have a positive charge [15]. These Ca<sup>+2</sup> s congregate between the contact surface and SBF. The ions measurement could describe possible biomolecule interaction in the apatite formation process [23, 29]. Sodium detection could enhance the mechanical stability of the apatite formation, according to Chitra and Balakumar [8]; besides, Na is also a key mineral and electrolyte for nerve and muscle function. Our findings suggest that Na/K substitutions could contribute in the mechanical stability of apatite biofouling activities on TNA nanosurface [13].

On the other hand, an implant failure is frequently associated with platelet biofouling that could negatively stimulate coagulation and thrombogenesis activities [4]. The surface of the blood-contacting biomaterial must not interact negatively with any blood components in order to be classified as non-haemolytic and anti-thrombogenic implantable material [5, 6]. RBCs are the most rigid cells in the blood; shear stress and changes in osmotic pressure can cause them to rupture and induce haemolysis especially involving external factors [7]. Findings from this study found neither Ti nor TNA showed any haemolysis sign. Platelets, on the other hand, are capable of swiftly recognizing external surfaces and initiating blood coagulation. Platelet adhesion is critical in stimulating coagulation factors for the haemostasis process in the human body [9]. The free haemoglobin produced from the rupture of the red blood cell is an important indicator for the clot clotting process. As the blood clots increases, the absorbance of the haemoglobin from red blood cell will decrease due to unable to form the clotting process. In this study, detrimental biofouling activities involving platelet and coagulant factors were not observed on TNA nanosurface.

In general, the presence of thrombin, fibrinogen in the platelet converts to fibrin, causing platelet adhesion when it comes into contact with any surface. When a platelet in the blood comes into contact with the material surface of a medical implant, the factor XII zymogen interacts with an unknown surface and converts prothrombin to thrombin [26]. When thrombin is present, fibrinogen is transformed into fibrin, which promotes the thrombin formation kinetics. Lower protein adsorption and less factor XII activation [25] are expected to reduce the clotting formation on material surface as observed in this study on TNA. Furthermore, prolonged APTT also indicates enhanced anticoagulant activity of the material, which is often used to assess the in vitro anticoagulant property of biomaterials [12]. The delay of clotting time can be considered due to enhanced surface roughness, especially on TNA nanosurface [21]. This coagulation tests could indicate the presence of anti-thrombogenic activity [17, 25]. In this study, TNA exhibits double-edged biofouling potentials that resist adverse biofouling qualities linked with thrombogenesis and haemolysis



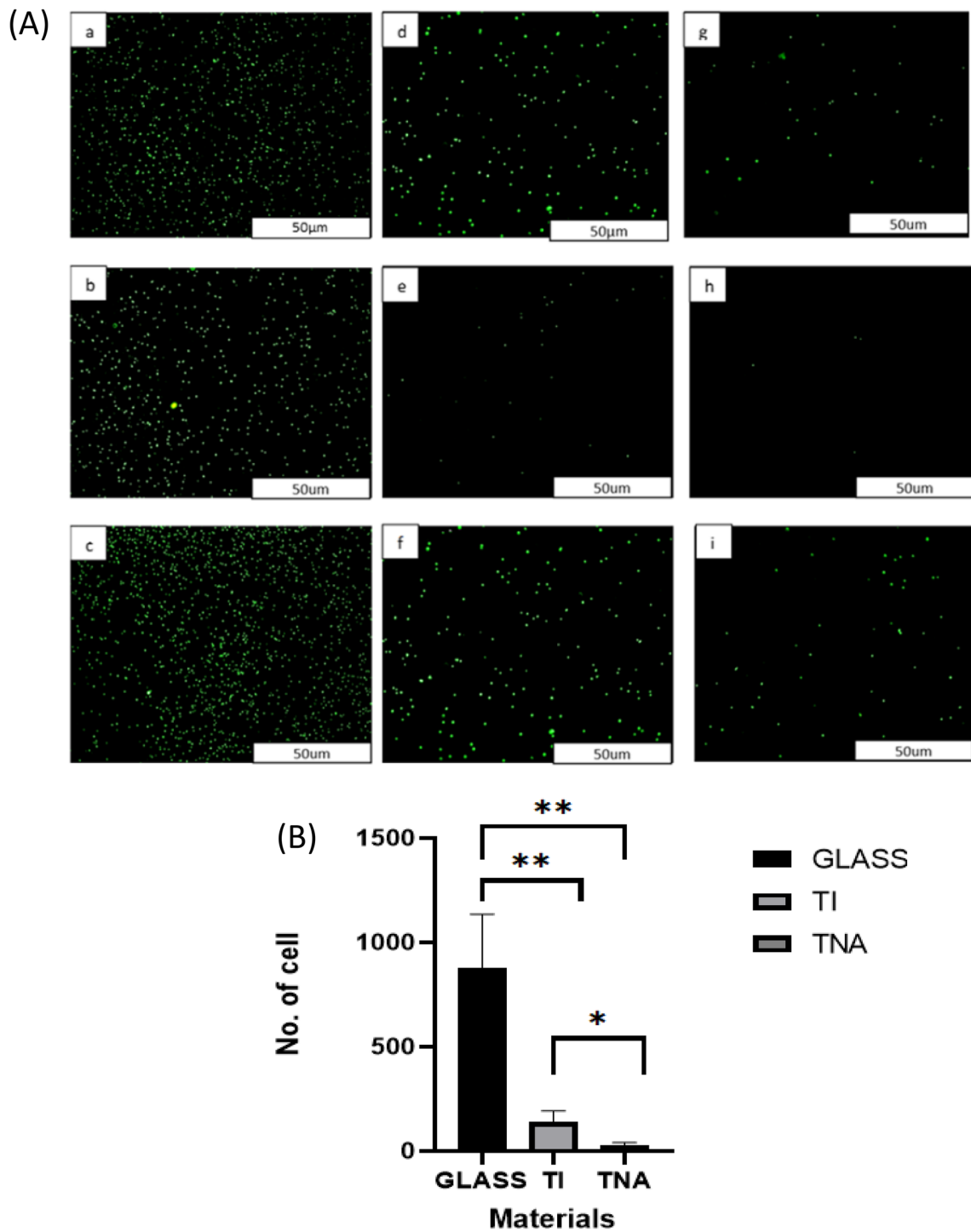


**Fig. 6** Platelet adhesion profile using fluorescence microscopy analysis on glass, Ti alloy, and TNA nanosurfaces. **A** The green signals represent the presence of adhered live cells (platelets and leukocytes) stained with calcein-AM staining. The image of (a–c) displayed observation on glass surface, (d–f) on the Ti surface, and (g–i) is on the TNA surface. Experiment were done in triplicate. **B** Quantitative data on the number of cells covered by the adhered cells on the surface using ImageJ software. The result shows significantly lower cell adhesion on TNA nanosurface when compared to glass ( $p = 0.0047$ ) and Ti alloy ( $p = 0.0218$ ). The error bar represents the standard deviation

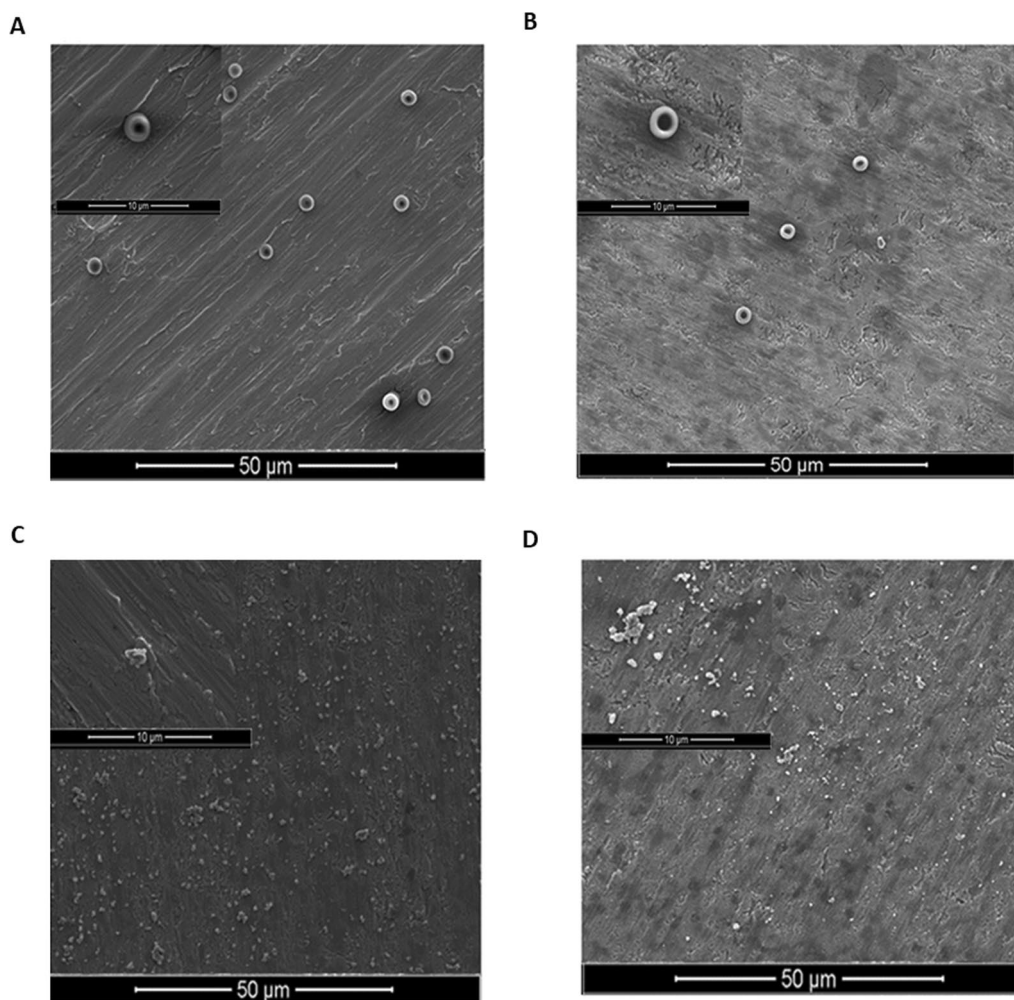


**Fig. 7** FESEM characterization on blood and platelet activation. **A** RBC aggregation on the surface of Ti, **B** RBC aggregation on TNA, **C** Platelet activation on Ti surface, and **D** platelet activation on the TNA surface. The FESEM image was captured at magnification 2000× (50 μm) and also 10,000× (10 μm)

risk, while positive biofouling on apatite deposition aids the osseointegration process.

### 5 Conclusion

In this work, the double-edged sword of biofouling properties of TNA nanosurface was described by apatite formation ability and less risk in thrombogenic activities involving platelet and coagulant factors. TNA nanosurface technology could involve a unique biofouling surface adhesion force, allowing selective substrate adherence that contributes in bio-, cyto-, and haemocompatibility properties. The hydrophilicity of the TNA also shows it has improved haemocompatibility compared to Ti alloy, which would be beneficial for medical implant surface technology.

### Abbreviations

SBF	Simulated body fluid
TNA	Titania nanotube arrays
Ti	Titanium
FESEM	Field emission scanning electron microscope
ICP-OES	Inductively coupled plasma-optical emission spectrometry
Na	Sodium
K	Potassium
P	Phosphorus
Ca	Calcium
EDTA	Ethylene diamine tetra-acetic acid
FBC	Full blood count
RBC	Red blood cell
Hb	Haemoglobin
PCV	Haematocrit
MCV	Mean cell volume
MCH	Mean corpuscular haemoglobin
MCHC	Mean corpuscular haemoglobin concentration
APTT	Activated partial thromboplastin clotting time

PT	Prothrombin time
PBS	Phosphate-buffered saline
OD	Optical densities
PRP	Platelet-rich plasma

### Acknowledgements

The authors would like to thank Universiti Sains Malaysia for sponsoring this work under research grant RUI EKSESAIS 2019 (No:1001/CIPPT/8012338).

### Author contributions

RM is the principal investigator who contributed in the concept, idea, experimental design, and writing process and gave final approval of this paper for publication. KP carried out all experimental works and prepared the manuscript. DW, RH, SN, NH, WE assisted in vitro and hemocompatibility work. SS guides in the material characterization procedures. All authors have given approval to the final version of the manuscript.

### Funding

The authors would like to thank Universiti Sains Malaysia (RUI EKSESAIS 2019 (No: 1001/CIPPT/8012338) for sponsoring this work.

### Availability of the data and materials

All data and set of results are applicable upon requests from the corresponding author on a reasonable request.

### Code availability

Not applicable.

### Declarations

#### Ethics approval and consent to participate

All procedures performed involving human participants followed The Human Research Ethics Committee of USM (JEPeM), approval no: 19110837 by: Jawatankuasa Etika Penyelidikan Manusia USM (JEPeM), Human Research Ethics Committee USM (HREC), Universiti Sains Malaysia, Kampus Kesihatan. 16150 Kubang Kerian, Kelantan, Malaysia. The consent had been achieved from the participants upon an understanding of the procedure performed. The protocol for all tests was approved by the JEPeM.

#### Consent for publication

All participants were informed and approached for publication.

#### Competing interests

All authors declared no conflict of interest.

#### Author details

<sup>1</sup>Department of Biomedical Science, Advanced Medical and Dental Institute, Universiti Sains Malaysia, 13200 Kepala Batas, Pulau Pinang, Malaysia. <sup>2</sup>Reading School of Pharmacy, Whiteknights, Reading RG6 6U, UK. <sup>3</sup>Department of Clinical Medicine, Advanced Medical and Dental Institute, Universiti Sains Malaysia, 13200 Kepala Batas, Pulau Pinang, Malaysia. <sup>4</sup>Neogenix Laboratoire Sdn Bhd, 81750 Masai, Johor, Malaysia. <sup>5</sup>Materials Technology Group, Industrial Technology Division, Nuclear Malaysia Agency, 43000 Bangi, Kajang, Selangor, Malaysia. <sup>6</sup>School of Materials and Mineral Resources Engineering, Universiti Sains Malaysia, Engineering Campus, 14300 Nibong Tebal, Seberang Perai Selatan, Pulau Pinang, Malaysia.

Received: 28 September 2022 Accepted: 14 February 2023

Published online: 03 April 2023

### References

- ASTM International (2013) Standard practice for assessment of hemolytic properties of materials. Practice. <https://doi.org/10.1520/F0756-13>. Copy right
- Abdal-hay A, Gulati K, Fernandez-Medina T, Qian M, Ivanovski S (2020) In situ hydrothermal transformation of titanium surface into lithium-doped continuous nanowire network towards augmented bioactivity. *Appl Surf Sci* 505:144604
- Baker EA, Fleischer MM, Vara AD, Salisbury MR, Baker KC, Fortin PT, Friedrich CR (2021) Local and systemic in vivo responses to osseointegrative titanium nanotube surfaces. *Nanomaterials* 11(3):583
- Becker K et al (2014) TiO<sub>2</sub> nanoparticles and bulk material stimulate human peripheral blood mononuclear cells. *Food Chem Toxicol* 65:63–69. <https://doi.org/10.1016/j.fct.2013.12.018>
- Blok LJS, Engels GE, van Oeveren W (2016) In vitro hemocompatibility testing: the importance of fresh blood. *Biointerphases* 11:029802. <https://doi.org/10.1116/1.4941850>
- Brandt E, Petersen F, Ludwig A, Ehler JE, Bock L, Chen J et al (2021) Photo-functionalized TiO<sub>2</sub> nanotubes decorated with multifunctional Ag nanoparticles for enhanced vascular biocompatibility. *Bioact Mater* 6(1):45–54. <https://doi.org/10.1016/j.bioactmat.2020.07.009>
- Chen LQ et al (2015) Nanotoxicity of silver nanoparticles to red blood cells: size-dependent adsorption, uptake, and hemolytic activity. *Chem Res Toxicol* 28(3):501–509. <https://doi.org/10.1021/tx500479m>
- Chitra S, Balakumar S (2021) Insight into the impingement of different sodium precursors on structural, biocompatible, and hemostatic properties of bioactive materials. *Mater Sci Eng: C* 123:111959. <https://doi.org/10.1016/j.msec.2021.111959>
- Choi J et al (2011) Physicochemical characterization and in vitro hemolysis evaluation of silver nanoparticles. *Toxicol Sci* 123(1):133–143. <https://doi.org/10.1093/toxic/kfr149>
- Chou Y-N, Venault A, Cho C-H, Sin M-C, Yeh L-C, Jheng-Fong J, Chinnathambi A, Chang Y, Yung C (2017) Epoxylated zwitterionic triblock copolymers grafted onto metallic surfaces for general biofouling mitigation. *Langmuir*. <https://doi.org/10.1021/acs.langmuir.7b02164>
- Effendy WNFWE, Mydin RBS, Gazzali AM, Sreekantan S (2020) Therapeutic nano-device: Study of biopolymer coating on titania nanotubes array loaded with chemodrug targeted for localized cancer therapy application. In: IOP Conference series: materials science and engineering, vol 932. IOP Publishing, p 012116
- Elahi MF, Guan G, Wang L (2014) Hemocompatibility of surface modified silk fibroin materials: a review. *Rev Adv Mater Sci* 38(2):148–159
- Esguerra-Arce A et al (2016) Influence of the Al content on the: In vitro bioactivity and biocompatibility of PVD Ti1-xAlxN coatings for orthopedic applications. *RSC Adv* 6(65):60756–60764. <https://doi.org/10.1039/c6ra08081b>
- Ferrer MCC, Eckmann UN, Composto RJ, Eckmann DM (2013) Hemocompatibility and biocompatibility of antibacterial biomimetic hybrid films. *Toxicol Appl Pharmacol* 272(3):703–712
- Goffredo GB, Accoroni S, Totti C, Romagnoli T, Valentini L, Munafò P (2016) Titanium dioxide based nanotreatments to inhibit microalgal fouling on building stone surfaces. *Build Environ* 112:209–222. <https://doi.org/10.1016/j.buildenv.2016.11.034>
- Jafari S, Mahyad B, Hashemzadeh H, Janfaza S, Gholikhani T, Tayebi L (2020) Biomedical applications of TiO<sub>2</sub> nanostructures: Recent advances. *Int J Nanomed* 15:3447. <https://doi.org/10.2147/IJN.S249441>
- Jaganathan SK, Mani MP, Ayyar M, Krishnasamy NP, Nageswaran G (2018) Blood compatibility and physicochemical assessment of novel nanocomposite comprising polyurethane and dietary carotino oil for cardiac tissue engineering applications. *J Appl Polym Sci* 135(3):45691
- Khandan A, Abdellahi M, Barenji RV, Ozada N, Karamian E (2015) Introducing natural hydroxyapatite-diopside (NHA-Di) nano-bioceramic coating. *Ceramics Int* 41(9):12355–12363
- Kokubo T, Yamaguchi S (2019) Simulated body fluid and the novel bioactive materials derived from it. *J Biomed Mater Res, Part A* 107(5):968–977
- Kurup A, Dhattrak P, Khasnis N (2021) Surface modification techniques of titanium and titanium alloys for biomedical dental applications: a review. *Mater Today: Proc* 39:84–90. <https://doi.org/10.1016/j.matpr.2020.06.163>
- Li JW et al (2012) The hemocompatibility and the reabsorption function of TiO<sub>2</sub> nanotubes biomembranes. *Chin Sci Bull* 57(16):2022–2028. <https://doi.org/10.1007/s11434-012-5038-x>
- Li X et al (2012) Biocompatibility and toxicity of nanoparticles and nanotubes. *J Nanomat*. <https://doi.org/10.1155/2012/548389>
- Li M et al (2016) Electrophoretic-deposited novel ternary silk fibroin/graphene oxide/hydroxyapatite nanocomposite coatings on titanium substrate for orthopedic applications. *Front Mater Sci* 10(3):270–280. <https://doi.org/10.1007/s11706-016-0347-7>

24. Liu H, Yang D, Yang H, Zhang H, Zhang W, Fang Y, Xi Z (2013) Comparative study of respiratory tract immune toxicity induced by three sterilisation nanoparticles: silver, zinc oxide and titanium dioxide. *J Hazard Mater* 248:478–486
25. Manivasagam VK, Popat KC (2020) In vitro investigation of hemocompatibility of hydrothermally treated titanium and titanium alloy surfaces. *ACS Omega* 5(14):8108–8120. <https://doi.org/10.1021/acsomega.0c00281>
26. Mohan CC, Chennazhi KP, Menon D (2013) In vitro hemocompatibility and vascular endothelial cell functionality on titania nanostructures under static and dynamic conditions for improved coronary stenting applications. *Acta Biomater* 9(12):9568–9577. <https://doi.org/10.1016/j.actbio.2013.08.023>
27. Mydin RBS, Hazan R, FaridWajidi MF, Sreekantan S (2018) Titanium dioxide nanotube arrays for biomedical implant materials and nanomedicine applications. In: Titanium dioxide: material for a sustainable environment. IntechOpen. <https://doi.org/10.5772/intechopen.73060>
28. Oyane A, Kim H-M, Furuya T, Kokubo T, Miyazaki T, Nakamura T (2003) Preparation and assessment of revised simulated body fluids 65A(2): 188–195. <https://doi.org/10.1002/jbm.a.10482>
29. Razavi M, Khandan A (2017) Safety, regulatory issues, long-term biotoxicity, and the processing environment. In *Nanobiomaterials science, development and evaluation*, Woodhead Publishing, pp 261–279
30. Sabino RM, Kauk K, Movafaghi S, Kota A, Popat KC (2019) Interaction of blood plasma proteins with superhemophobic titania nanotube surfaces. *Nanomed: Nanotechnol Biol Med* 21:102046
31. Schuster JM, Schvezov CE, Rosenberger MR (2015) Influence of experimental variables on the measure of contact angle in metals using the sessile drop method. *Proc Mater Sci* 8:742–751
32. Weber M, Steinle H, Golombek S, Hann L, Schlensak C, Wendel HP, Avci-Adali M (2018) Blood-contacting biomaterials: in vitro evaluation of the hemocompatibility. *Front Bioeng Biotechnol* 1:10. <https://doi.org/10.3389/fbioe.2018.0009>

### Publisher's Note

Springer Nature remains neutral with regard to jurisdictional claims in published maps and institutional affiliations.

Submit your manuscript to a SpringerOpen<sup>®</sup> journal and benefit from:

- Convenient online submission
- Rigorous peer review
- Open access: articles freely available online
- High visibility within the field
- Retaining the copyright to your article

---

Submit your next manuscript at ► [springeropen.com](https://www.springeropen.com)

---